

The Magnetic Predissociation of the $B^3\Pi_{0+u}$ State of the Iodine Molecule

Masaaki BABA,* Misako KIMURA, Toshiyuki TSUBOI, Hajime KATÔ,
and Saburo NAGAKURA†

Department of Chemistry, Faculty of Science, Kobe University, Nada-ku, Kobe 657

†Institute for Molecular Science, Myodaiji, Okazaki 444

(Received July 4, 1988)

It is shown that the predissociation of I_2 excited to the $B^3\Pi_{0+u}$ state can occur through the coupling with the $2431^1\Pi_u$ state by gyroscopic and Zeeman interactions. The interaction matrix elements between the $B^3\Pi_{0+u}$ and $2431^1\Pi_u$ states are shown to be nonzero, for the $2431^1\Pi_u$ state is mixed significantly with the $2431^3\Pi_{1u}$ state by the spin-orbit interaction. The v, J dependence of the magnetic-quenching ratios of the $B^3\Pi_{0+u}-X^1\Sigma_g^+$ fluorescence intensity has been measured and analyzed. The rate constants of the magnetic predissociation in the $B^3\Pi_{0+u}$ state have also been evaluated. The magnetic-field dependence of the hyperfine structure has been measured by means of the Doppler-free intermodulated fluorescence method.

In 1913, Steubing¹⁾ found the quenching of the $B^3\Pi_{0+u}-X^1\Sigma_g^+$ fluorescence by an external magnetic field. Turner²⁾ suggested that it was due to magnetic predissociation in the $B^3\Pi_{0+u}$ state. Van Vleck³⁾ suggested that the mixing of the $B^3\Pi_{0+u}$ state with the repulsive $^3\Pi_{0-u}$ state causes the magnetic predissociation. The rate constants were determined by studies of the magnetic quenching of the fluorescence intensity.^{4,5)}

The natural predissociation (predissociation in a zero magnetic field) of the $B^3\Pi_{0+u}$ state was found by analyzing the fluorescence lifetime and the absorption strength.^{6–9)} The vibrational quantum-number dependence of the natural predissociation was very similar to that of the magnetic predissociation. The predissociation was attributed to the gyroscopic interaction (heterogeneous electronic-rotational perturbation) and the hyperfine interaction between the $B^3\Pi_{0+u}$ and $2431^1\Pi_u$ states.¹⁰⁾ Vigue et al.^{11,12)} found an interference effect between the natural and magnetic predissociations. Both the natural and magnetic predissociations in the $B^3\Pi_{0+u}$ state were consequently assigned as originating from the coupling with the $2431^1\Pi_u$ state.¹²⁾ However, this study is not yet complete because the matrix elements of the coupling between the $^3\Pi_{0+u}$ and $^1\Pi_u$ states have been calculated to be zero for the gyroscopic and Zeeman interactions.

In this paper, we shall show that the matrix elements of the Zeeman interaction between the $B^3\Pi_{0+u}$ and $2431^1\Pi_u$ states are not zero, for the $2431^1\Pi_u$ state is mixed with the $2431^3\Pi_{1u}$ state by the spin-orbit coupling.^{13,14)} We have measured the magnetic quenching ratios of completely resolved rotational lines. By using these results and the fluorescence lifetime,¹²⁾ we shall reexamine the rate constants of the magnetic predissociation in the $B^3\Pi_{0+u}$ state. The magnetic-field dependence of the hyperfine structure has been measured by the Doppler-free intermodulated fluorescence method; these results shall also be discussed.

Experimental

A single-mode tunable ring dye laser equipped with an autoscanner system (Coherent 699-29) was used for excitation. A small amount of solid iodine was sealed in a Pyrex cell after trap-to-trap purifications. The residual gas pressure was lower than 1×10^{-5} Torr (1 Torr \approx 133.322 Pa). The vapour pressure of the iodine was controlled by cooling the sidearm of the cell. The cell was placed in the center of an electric magnet. The laser light was linearly polarized and propagated with its polarization parallel to the applied magnetic field. The fluorescence was detected by a photomultiplier (Hamamatsu R712) through a glass filter (Toshiba R66) to block the scattered laser light. The output of the photomultiplier was phase-sensitively detected through a lock-in amplifier (PAR Model 128) by chopping the laser light at 960 Hz.

The magnetic-quenching ratio for a rotational level was determined by measuring the change in the peak intensity with the applied magnetic field. The Doppler-limited line shape did not change with the magnetic field. Therefore, the height of the maximum intensity was proportional to the integrated line intensity. The assignment of the rotational line was carried out using the molecular constants obtained by Luc.¹⁵⁾

The hyperfine structure was observed by means of the intermodulated fluorescence method.¹⁶⁾ The laser light was split into two counter propagating beams which were chopped at 390 Hz and 570 Hz and which crossed in the center of the cell. We obtained the Doppler-free spectrum by detecting the fluorescence intensity at 960 Hz through a lock-in amplifier. The linewidth was about 10 MHz at the laser power of 30 mW mm⁻² and the vapour pressure of 30 mTorr (with the sidearm cooled at 0 °C).

Theoretical

As Mulliken defined,¹⁴⁾ we shall denote the MO (molecular orbital) electronic configuration of the valence-shell state of the $\sigma_g^2\sigma_u^2\sigma_g^m\pi_u^p\pi_g^q\sigma_u^n$ type with $m+n+p+q=10$ as $mpqn$. The basic determinant wavefunctions of the iodine molecule are given by:

$$\begin{aligned} |2440^1\Sigma_g^+> &= |\pi_{g+1}\bar{\pi}_{g+1}\pi_{g-1}\bar{\pi}_{g-1}|, \\ |2431^3\Pi_{0+u}> &= (2)^{-1/2}(|\pi_{g+1}\pi_{g-1}\bar{\pi}_{g-1}\sigma_u| \end{aligned}$$

$$\begin{aligned}
& + |\pi_{g+1}\bar{\pi}_{g+1}\bar{\pi}_{g-1}\bar{\sigma}_u|, \\
|2431^3\Pi_{1u+}\rangle &= (2)^{-1/2}(|\pi_{g+1}\bar{\pi}_{g+1}\pi_{g-1}\bar{\sigma}_u| \\
& + |\pi_{g+1}\bar{\pi}_{g+1}\bar{\pi}_{g-1}\sigma_u|), \\
|2431^3\Pi_{1u-}\rangle &= (2)^{-1/2}(|\pi_{g+1}\pi_{g-1}\bar{\pi}_{g-1}\bar{\sigma}_u| \\
& + |\pi_{g+1}\pi_{g-1}\bar{\pi}_{g-1}\sigma_u|), \\
|2431^1\Pi_{1u+}\rangle &= (2)^{-1/2}(|\pi_{g+1}\bar{\pi}_{g+1}\pi_{g-1}\bar{\sigma}_u| \\
& - |\pi_{g+1}\bar{\pi}_{g+1}\bar{\pi}_{g-1}\sigma_u|), \\
|2431^1\Pi_{1u-}\rangle &= (2)^{-1/2}(|\pi_{g+1}\pi_{g-1}\bar{\pi}_{g-1}\bar{\sigma}_u| \\
& - |\pi_{g+1}\pi_{g-1}\bar{\pi}_{g-1}\sigma_u|),
\end{aligned} \quad (1)$$

where MO without a bar indicates with an α -spin, where MO with a bar indicates with a β -spin, and where a determinant such as $|\sigma_g(1)\bar{\sigma}_g(2)\pi_{u+}(3)\bar{\pi}_{u+}(4)\pi_{u-}(5)\bar{\pi}_{u-}(6)\pi_{g+}(7)\bar{\pi}_{g+}(8)\pi_{g-}(9)\bar{\pi}_{g-}(10)| / (10!)^{1/2}$ is briefly denoted as $|\pi_{g+1}\bar{\pi}_{g+1}\pi_{g-1}\bar{\pi}_{g-1}|$ in Eq. 1 by omitting the common MOs of a low energy. MOs $\pi_{g\pm 1}$ and σ_u in Eq. 1 are, respectively, of the form $5p_{\pm 1}-5p_{\pm 1}$ and $5p_0+5p_0$, where $5p_0=5p_z$ and $5p_{\pm 1}=\mp 2^{-1/2}(5p_x \pm i5p_y)$.

As a set of basis functions, we use wavefunctions of simple products, $|A\rangle|S\Sigma\rangle|v\rangle|J\Omega M\rangle$. The function $|A\rangle|S\Sigma\rangle|v\rangle$ is a wavefunction for a nonrotating molecule, where A and Σ represent the projections of the total electronic orbital and the total electronic spin angular momenta along the molecular axis respectively, while v represents the vibrational quantum number. All of these are expressed in molecule-fixed coordinates. The wavefunction $|J\Omega M\rangle$ associated with the molecular rotation is expressed in laboratory-fixed coordinates, where the quantum numbers J and M specify the total angular momentum and its projection along the laboratory-fixed Z axis respectively and where $\Omega=A+\Sigma$. The eigenfunctions for the levels of the unperturbed states $2440^1\Sigma_g^+$, $2431^3\Pi_{0+u}$, $2431^3\Pi_{1u}$, and $2431^1\Pi_{1u}$, are expressed, respectively, as:¹⁷⁾

$$\begin{aligned}
|2440^1\Sigma_g^+vJM\rangle &= |0+\rangle|00\rangle|v\rangle|J0M\rangle, \\
|2431^3\Pi_{0+u}vJM\rangle &= |0+\rangle|10\rangle|v\rangle|J0M\rangle, \\
|2431^3\Pi_{1u\pm}vJM\rangle &= 2^{-1/2}(|1\rangle|10\rangle|v\rangle|J1M\rangle \\
&\pm |-1\rangle|10\rangle|v\rangle|J-1M\rangle), \\
|2431^1\Pi_{1u\pm}vJM\rangle &= 2^{-1/2}(|1\rangle|00\rangle|v\rangle|J1M\rangle \\
&\pm |-1\rangle|00\rangle|v\rangle|J-1M\rangle),
\end{aligned} \quad (2)$$

where the electronic wavefunctions $|0+\rangle|00\rangle$, $|0+\rangle|10\rangle$, $|1\rangle|10\rangle$, $|-1\rangle|10\rangle$, $|1\rangle|00\rangle$, and $|-1\rangle|00\rangle$ are equal to $|2440^1\Sigma_g^+\rangle$, $|2431^3\Pi_{0+u}\rangle$, $|2431^3\Pi_{1u+}\rangle$, $|2431^3\Pi_{1u-}\rangle$, $|2431^1\Pi_{1u+}\rangle$, and $|2431^1\Pi_{1u-}\rangle$ of Eq. 1, respectively.

The spin-orbit interaction induces a mixing of the singlet and triplet wavefunctions, and it occurs between the same J levels. The perturbed wavefunctions of I_2 at the equilibrium distance R_e of the ground state were calculated by Mulliken¹⁴⁾ as:

$$\begin{aligned}
|X^1\Sigma_g^+vJM\rangle &= |2440^1\Sigma_g^+vJM\rangle \\
&- 0.153|2341^3\Pi_{0+g}vJM\rangle, \\
|B^3\Pi_{0+u}vJM\rangle &= 0.916|2431^3\Pi_{0+u}vJM\rangle \\
&- 0.378|1342^3\Pi_{0+u}vJM\rangle
\end{aligned}$$

$$\begin{aligned}
|A^3\Pi_{1u\pm}vJM\rangle &= -0.064|1441^1\Sigma_u^+vJM\rangle, \\
&= 0.908|2431^3\Pi_{1u\pm}vJM\rangle \\
&+ 0.419|2431^1\Pi_{1u\pm}vJM\rangle, \\
|2431^1\Pi_{1u\pm}vJM\rangle &= 0.419|2431^3\Pi_{1u\pm}vJM\rangle \\
&- 0.908|2431^1\Pi_{1u\pm}vJM\rangle.
\end{aligned} \quad (3)$$

The magnetic field was applied along the Z -axis in laboratory-fixed coordinates. The basic electronic orbital and spin wavefunctions are expressed in molecule-fixed coordinates. The Zeeman interaction energy in the molecule-fixed coordinates is written as:¹⁷⁾

$$H_Z = -[2^{-1/2}(\mu_+D_{01}^1 - \mu_-D_{0-1}^1) + \mu_zD_{00}^1]H, \quad (4)$$

where H is the magnetic field. $\mu_+ = -\mu_B\sum_i(l_+ + 2s_+)_i$, $\mu_- = -\mu_B\sum_i(l_- + 2s_-)_i$, and $\mu_z = -\mu_B\sum_i(l_z + 2s_z)_i$ are the components of the magnetic moment of the molecule, and D_{MN}^J is the rotation matrix. We shall always use the representations of the rotation group, the angular momenta, the coupling coefficients, and the tensors as defined by Brink and Satchler.¹⁸⁾ The matrix element of the Zeeman interaction is zero between different spin states in Eq. 2, while the nonzero matrix elements for $|2431^3\Pi_{0+u}v'JM\rangle$ are calculated to be:

$$\begin{aligned}
\langle 2431^3\Pi_{0+u}v'JM|H_Z|2431^3\Pi_{1u-v}J-1M\rangle &= 4\mu_B H \langle v'|v\rangle [(J-1)(J-M)(J+M)/2J(2J-1)(2J+1)]^{1/2}, \\
\langle 2431^3\Pi_{0+u}v'JM|H_Z|2431^3\Pi_{1u+v}JM\rangle &= 4\mu_B H \langle v'|v\rangle M/[2J(J+1)]^{1/2}, \\
\langle 2431^3\Pi_{0+u}v'JM|H_Z|2431^3\Pi_{1u-v}J+1M\rangle &= -4\mu_B H \langle v'|v\rangle [(J+2)(J+1-M)(J+1+M) \\
&/ 2(J+1)(2J+1)(2J+3)]^{1/2}.
\end{aligned} \quad (5)$$

Thus, the $2431^3\Pi_{0+u}$ state can couple with the $2431^3\Pi_{1u}$ state by the Zeeman interaction. The Zeeman interaction between the $B^3\Pi_{0+u}$ and $2431^1\Pi_{1u}$ states has nonvanishing matrix elements, as can be seen from Eqs. 3 and 5.

The Hamiltonian of the gyroscopic interaction is written as:

$$H_G = -(\hbar^2/2\mu R^2)(J_+L_- + J_-L_+), \quad (6)$$

where μ is the reduced mass and where R is the internuclear distance. It causes perturbation between states that differ by $\Delta\Omega=\Delta A=\pm 1$ and $\Delta S=0$. The gyroscopic interaction between the $B^3\Pi_{0+u}$ and $2431^1\Pi_{1u}$ states arises through the nonzero matrix element:

$$\begin{aligned}
\langle 2431^3\Pi_{0+u}v'JM|H_G|2431^3\Pi_{1u+v}JM\rangle &= \\
&- G \langle v'|v\rangle [\hbar^2/2\mu R^2]v[J(J+1)]^{1/2},
\end{aligned} \quad (7)$$

where G is defined as $\langle 0+|L_-|1\rangle = \langle 0+|L_+|-1\rangle = 2^{-1/2}G$. The predissociation of I_2 excited to the $|B^3\Pi_{0+u}v'JM\rangle$ level can occur through the gyroscopic interaction

with the $|2431^1\Pi_{u+v}JM\rangle$ level; the rate is proportional to:

$$G^2 \langle v' | \hbar^2 / 2\mu R^2 | v \rangle^2 J(J+1). \quad (8)$$

In the presence of the magnetic field H along the Z axis, the predissociation of I_2 excited to the $|B^3\Pi_{0+u}v'JM\rangle$ level can occur through the Zeeman interaction with the $|2431^1\Pi_{u-v}J-1M\rangle$, $|2431^1\Pi_{u+v}JM\rangle$, and $|2431^1\Pi_{u-v}J+1M\rangle$ levels, as can be seen from Eqs. 3 and 5. The predissociation through the interaction between the $|B^3\Pi_{0+u}v'JM\rangle$ and $|2431^1\Pi_{u+v}JM\rangle$ levels can occur by both gyroscopic and Zeeman interactions. The rate of predissociation from the excited level $|B^3\Pi_{0+u}v'JM\rangle$ is proportional to:

$$\begin{aligned} & 8\mu_B^2 H^2 \langle v' | v \rangle^2 J(J-1)(J-M)(J+M) / J(2J-1)(2J+1) \\ & + |4\mu_B H \langle v' | v \rangle M [2J(J+1)]^{-1/2} \\ & - G \langle v' | \hbar^2 / 2\mu R^2 | v \rangle^2 J(J+1)^{1/2} \\ & + 8\mu_B^2 H^2 \langle v' | v \rangle^2 (J+2)(J+1-M)(J+1+M) \\ & / (J+1)(2J+1)(2J+3) = k_{p(M)}. \end{aligned} \quad (9)$$

The $B^3\Pi_{0+u} - X^1\Sigma_g^+$ transition is allowed through the nonvanishing transition moments of $\langle ^3\Pi_{0+u} | \mu | ^3\Pi_{0+g} \rangle$ and $\langle ^1\Sigma_u^+ | \mu | ^1\Sigma_g^+ \rangle$, where μ is an electric dipole moment. The dependence on J and M is the same for both these transition moments. For an excitation by a plane-polarized light with the electric vector along the Z axis, which is the case in our experiment, the nonvanishing moment of the $B^3\Pi_{0+u}(v'JM) - X^1\Sigma_g^+(v''JM)$ transition is given by:

$$\begin{aligned} & \langle B^3\Pi_{0+u}v'JM | \mu_z | X^1\Sigma_g^+v''J-1M \rangle \\ & = \mu(B-X) \langle v' | v'' \rangle [(J-M)(J+M) / (2J-1)(2J+1)]^{1/2}, \\ \text{and } & \langle B^3\Pi_{0+u}v'JM | \mu_z | X^1\Sigma_g^+v''J+1M \rangle \\ & = \mu(B-X) \langle v' | v'' \rangle [(J+1-M)(J+1+M) / \\ & (2J+1)(2J+3)]^{1/2}, \end{aligned} \quad (10)$$

where $\mu(B-X)$ is the electric dipole transition moment of the $B^3\Pi_{0+u} - X^1\Sigma_g^+$ transition.

The rate of the predissociation following the optical excitation is proportional to:

$$\begin{aligned} k_p &= (2J+1)^{-1} \sum_M k_{p(M)} \mu(B-X)^2 \langle v' | v'' \rangle^2 \\ & \times [(J-M)(J+M) / (2J-1)(2J+1) \\ & + (J+1-M)(J+1+M) / (2J+1)(2J+3)], \end{aligned} \quad (11)$$

The summation over M is equal to averaging over the molecular orientation; one thus obtains:

$$k_p = \mu(B-X)^2 \langle v' | v'' \rangle^2 [16\mu_B^2 H^2 \langle v' | v \rangle^2 J(J+1)(11J-5) / (2J-1)(2J+3) + G^2 \langle v' | \hbar^2 / 2\mu R^2 | v \rangle^2 J(J+1)/3], \quad (12)$$

where the first term is the contribution from the Zeeman interaction, while the second term is that from the gyroscopic interaction. It should be noted that the interference term disappears upon the averaging; hence, the interference can not be observed in our

experiment. Accordingly, the rate of predissociation due to the Zeeman interaction can be written as:

$$k_{mpr} = bH^2, \quad (13)$$

while the rate of predissociation due to the gyroscopic interaction can be written as:

$$k_{gpr} = gJ(J+1), \quad (14)$$

where b and g are constants.

Experimental Results and Discussion

A portion of the fluorescence excitation spectrum of the iodine molecule, which includes the band origin of the $B^3\Pi_{0+u}(v'=6) - X^1\Sigma_g^+(v''=4)$ transition, is shown in Fig. 1. Most of the lines are rotationally resolved and can be easily assigned. However, the hyperfine structure is not resolved because of the Doppler-width. We measured the magnetic quenching ratio of the line intensity of each rotational level. Since the lifetime of the $B^3\Pi_{0+u}$ state is relatively long (an order of $\sim \mu s$), the fluorescence intensity is sensitive to optical saturation and molecular collisions. Therefore, the measurement should be made at as low a laser power and as low a vapour pressure as possible. All the measurements were carried out at 1 mW mm⁻² and 30 mTorr; it was thus confirmed that the quenching ratio under these conditions was almost independent of the laser power.

We also measured the magnetic-quenching ratio I_H/I_0 of each rotational line, where I_H and I_0 are, respectively, the fluorescence intensity at the magnetic

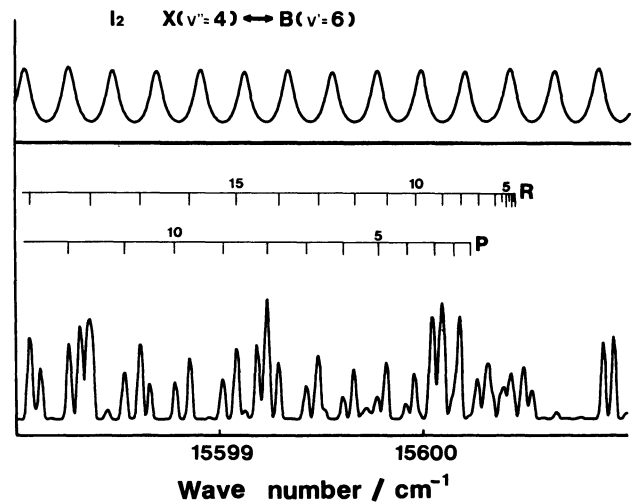


Fig. 1. Fluorescence excitation spectrum of I_2 around the band origin of the $B^3\Pi_{0+u}(v'=6) - X^1\Sigma_g^+(v''=4)$ transition. The assignment of each rotational line is shown above. The upper trace is the transmittance of the etalon (FSR=6.5 GHz) which is monitored to confirm the linearity of the scan and to detect a mode-hop of the laser line.

field H and at the zero magnetic field. The observed values of I_H/I_0 for $J'=20-80$ levels of $v'=6$ and 10 at $H=0.78$ and 1.67 T are shown in Fig. 2. The magnetic quenching ratio depends on the decay rate of the J' level. Hence, the values of the P and R lines of the

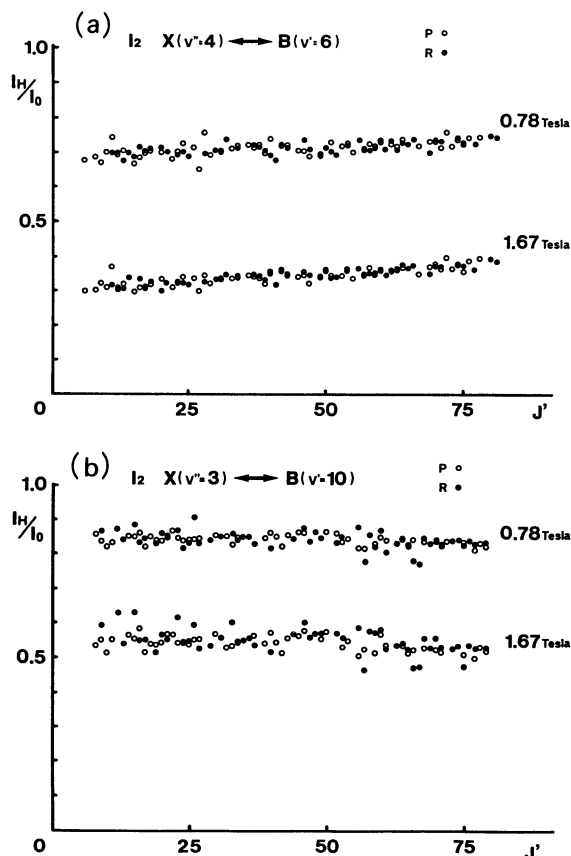


Fig. 2. The values of I_H/I_0 for J' levels of $B^3\Pi_{0^+u}(v'=6)$ at the magnetic field of 0.78 and 1.67 T are shown in (a). Those for J' levels of $B^3\Pi_{0^+u}(v'=10)$ are shown in (b).

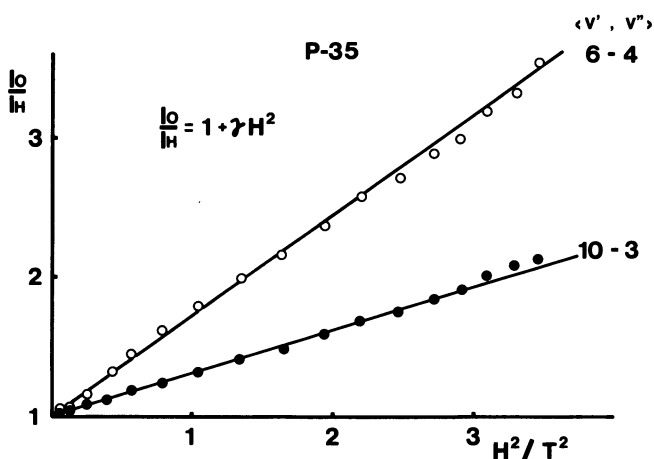


Fig. 3. Magnetic field dependence of the quenching ratio I_0/I_H of the P(35) lines of the $B^3\Pi_{0^+u}(v'=6)-X^1\Sigma_g^+(v''=4)$ and $B^3\Pi_{0^+u}(v'=10)-X^1\Sigma_g^+(v''=3)$ transitions.

identical J' are naturally the same. We measured the magnetic-field dependence of the quenching ratio for each rotational line. The ratios I_0/I_H of the P(35) lines of the $B^3\Pi_{0^+u}(v'=6)-X^1\Sigma_g^+(v''=4)$ and $B^3\Pi_{0^+u}(v'=10)-X^1\Sigma_g^+(v''=3)$ transitions are plotted against the square of the applied magnetic field in Fig. 3. The experimental error was $\pm 1\%$.

The magnetic-quenching ratio of the fluorescence is expressed as:

$$I_H/I_0 = (k_{\text{rad}} + k_{\text{col}} + k_{\text{npr}}) / (k_{\text{rad}} + k_{\text{col}} + k_{\text{npr}} + k_{\text{mpr}}), \quad (15)$$

where k_{rad} , k_{col} , and k_{mpr} are, respectively, the rate of radiative decay, the rate of collisional quenching, and the rate of magnetic predissociation. k_{npr} is the rate of the natural predissociation, which is the sum of the rate of the gyroscopic predissociation k_{gpr} and the rate of the hyperfine predissociation k_{hpr} . The lifetime τ in the zero field is given by:

$$\tau = (k_{\text{rad}} + k_{\text{col}} + k_{\text{npr}})^{-1}. \quad (16)$$

From Eqs. 13, 15, and 16, one obtains:

$$I_0/I_H = 1 + \tau b H^2 = 1 + \gamma H^2. \quad (17)$$

One can determine the value of γ from the slope of I_0/I_H vs. H^2 . We measured the J dependence of the magnetic-quenching ratios for various v' levels. The

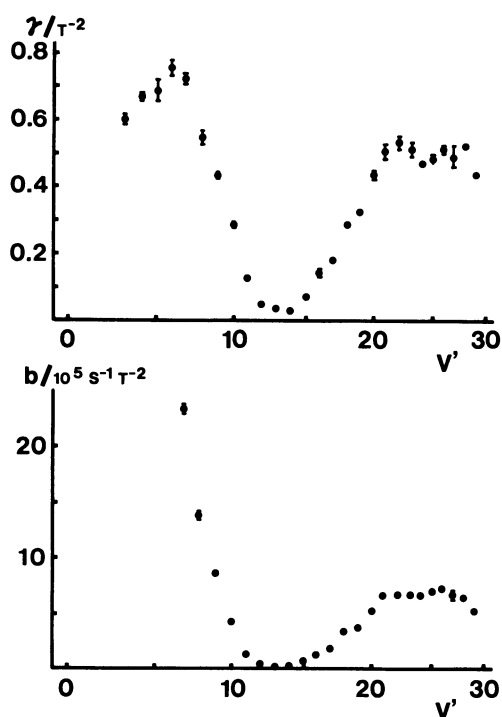


Fig. 4. Upper (a): Observed values of γ extrapolated to $J=0$ for various v levels. Lower (b): b values deduced from the observed γ values and the fluorescence lifetime at $J=0$ from Ref. 12.

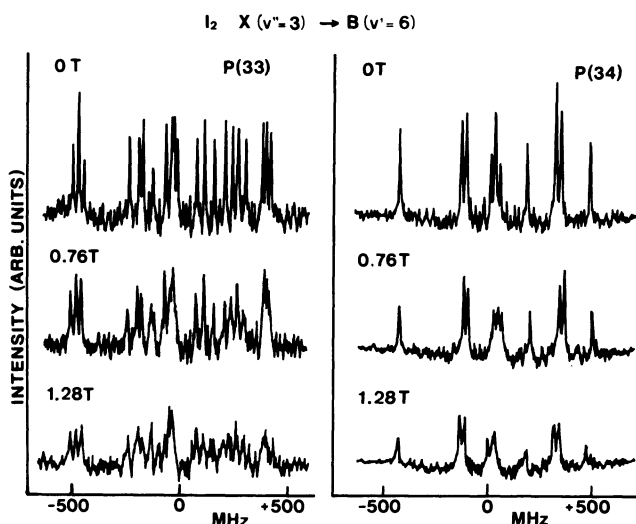


Fig. 5. Hyperfine structure of P(33) and P(34) lines of the $B^3\Pi_{0+u}(v'=6)-X^1\Sigma_g^+(v''=3)$ transition, and the change with the magnetic field.

results of the extrapolation of the values of γ at $J=0$ are shown in Fig. 4(a). At $J=0$, the rate of the gyroscopic predissociation is zero. We evaluated the values of τ at $J=0$ by using the results obtained by Vigue et al.¹²⁾ Unfortunately, their results are limited for $v' > 7$. Consequently we could obtain the b value at $J=0$ for $v'=7-29$; the b value obtained for each v' level is plotted in Fig. 4(b). The profile is very similar to that presented by Chapman et al.⁵⁾ and Vigue et al.,¹²⁾ but the absolute values are considerably different. We measured the magnetic-quenching ratio for many more rotationally resolved lines; hence, we could obtain more accurate values than the previous ones.

By using the intermodulated fluorescence technique,¹⁶⁾ we observed the hyperfine structure and the change with the magnetic field. The results for the P(33) and P(34) lines of the $B^3\Pi_{0+u}(v'=6)-X^1\Sigma_g^+(v''=3)$ transition are shown in Fig. 5. The Pauli exclusion principle requires that odd J levels of the $B^3\Pi_{0+u}$ state of $^{127}\text{I}_2$ can combine only with states of an even total nuclear spin ($I=0, 2$, and 4), while even J levels can combine only with states of an odd total nuclear spin ($I=1, 3$, and 5). Hence, 15 sublines are observed for an even J'' line and 21 sublines for an odd J'' line. In either the presence or absence of a magnetic field, no energy shift or line splitting of the hyperfine lines was observed. However, when a magnetic field was applied, a remarkable decrease of the intensity of each line was observed; the ratio of the change was almost the same for all lines.

The hyperfine structure could be explained by the nuclear electric quadrupole interaction and the nuclear spin-rotation interaction.^{20,21)} For a large value of $J(\gg I)$, the angular momentum J is almost parallel to $F=J+I$. The Zeeman interaction energy

with the nuclear spins may be expressed by:

$$E_{NZ} = g_1 \mu_N (M_1 + M_2) H, \quad (19)$$

where M_i is the projection of the nuclear spin angular momentum of the nucleus i along the molecular-fixed z axis. g_1 is a nuclear g -factor, and μ_N is the nuclear magneton. We used a linearly polarized light whose polarization was parallel to the magnetic field; hence, the transitions of $M'_F - M''_F = 0$ are allowed by an electric dipole transition. The nuclear g -factors of the $B^3\Pi_{0+u}$ and $X^1\Sigma_g^+$ states can be estimated to be almost the same, for no energy shift or line splitting of the hyperfine lines was observed when a magnetic field was applied.

Levenson and Schawlow²¹⁾ found that the nuclear spin-rotation interaction varied strongly with the vibrational quantum number v' of the $B^3\Pi_{0+u}$ state. The coupling was found to increase rapidly near the dissociation limit of the $B^3\Pi_{0+u}$ state. Broyer et al.²²⁾ found that the lifetime extrapolated to $J=0$ shows a strong variation with v , very similar to that of b . They assigned the origin of this new predissociation to the hyperfine predissociation. In order to make this problem clear, more extensive studies of Doppler-free spectroscopy by using a molecular beam will be necessary.

A part of this work was supported by the Joint Studies Program (1987–1988) of the IMS. H. K. and M. B. wish to thank the Ministry of Education of Japan for a Grant-in-Aid for scientific research.

References

- 1) W. Steubing, *Verh. d. D. Phys. Ges.*, **15**, 1181 (1913).
- 2) L. A. Turner, *Z. Phys.*, **65**, 464 (1930).
- 3) J. H. Van Vleck, *Phys. Rev.*, **40**, 344 (1932).
- 4) E. O. Degenkolb, J. I. Steinfeld, E. Wasserman, and W. Klemperer, *J. Chem. Phys.*, **51**, 615 (1969).
- 5) G. D. Chapman and P. R. Bunker, *J. Chem. Phys.*, **57**, 2951 (1972).
- 6) A. Chutjian, J. K. Link, and C. Brewer, *J. Chem. Phys.*, **46**, 2666 (1967).
- 7) A. Chutjian and T. C. James, *J. Chem. Phys.*, **51**, 1242 (1969).
- 8) J. Tellinghuisen, *J. Chem. Phys.*, **57**, 2397 (1972).
- 9) J. Tellinghuisen, *J. Chem. Phys.*, **58**, 2821 (1973).
- 10) M. Broyer, J. Vigue, and J. C. Lehmann, *J. Chem. Phys.*, **63**, 5428 (1975).
- 11) J. Vigue, M. Broyer, and J. C. Lehmann, *J. Chem. Phys.*, **62**, 4941 (1974).
- 12) J. Vigue, M. Broyer, and J. C. Lehmann, *J. Phys. (Paris)*, **42**, 937, 949, 961 (1981).
- 13) R. S. Mulliken, *Phys. Rev.*, **57**, 500 (1940).
- 14) R. S. Mulliken, *J. Chem. Phys.*, **55**, 288 (1971).
- 15) P. Luc, *J. Mol. Spectrosc.*, **80**, 41 (1980).
- 16) M. S. Sorem and A. L. Shawlow, *Opt. Comm.*, **5**, 148 (1972).
- 17) H. Katô, M. Baba, and I. Hanazaki, *J. Chem. Phys.*, **80**,

3936 (1984).

18) D. M. Brink and G. R. Satchler, *Angular Momentum*, Oxford University, Oxford, 1968.

19) G. A. Capella and H. P. Broida, *J. Chem. Phys.*, **58**, 4212 (1973).

20) M. Kroll, *Phys. Rev. Lett.*, **23**, 631 (1969).

21) M. D. Levenson and A. L. Schawlow, *Phys. Rev.*, **A6**, 10 (1972).

22) M. Broyer, J. Vigue, and J. C. Lehmann, *J. Chem. Phys.*, **64**, 4793 (1976).
